

Liraglutide Prevents Hypoadiponectinemia-Induced Insulin Resistance and Alterations of Gene Expression Involved in Glucose and Lipid Metabolism

Ling Li,¹ Zongyu Miao,¹ Rui Liu,² Mengliu Yang,² Hua Liu,³ and Gangyi Yang²

¹Key Laboratory of Diagnostic Medicine (Ministry of Education) and Department of Clinical Biochemistry, Chongqing Medical University College of Laboratory Medicine, Chongqing, China; ²Department of Endocrinology, the Second Affiliated Hospital, Chongqing Medical University, Chongqing, China; and ³Department of Pediatrics, University of Mississippi Medical Center, Jackson, Mississippi, United States of America

Liraglutide is a glucagonlike peptide (GLP)-1 analog that reduces blood glucose levels, increases insulin secretion and improves insulin sensitivity through mechanisms that are not completely understood. Therefore, we aimed to evaluate the metabolic impact and underlying mechanisms of liraglutide in a hypoadiponectinemia and high-fat diet (HFD)-induced insulin resistance (IR) model. Adiponectin gene targeting was achieved using adenovirus-transduced RNAi and was used to lower plasma adiponectin levels. Liraglutide (1 mg/kg) was given twice daily for 8 wks to HFD-fed apolipoprotein (Apo)E^{-/-} mice. Insulin sensitivity was examined by a hyperinsulinemic-euglycemic clamp. Gene mRNA and protein expressions were measured by quantitative real-time polymerase chain reaction (PCR) and Western blot, respectively. Administration of liraglutide prevented hypoadiponectinemia-induced increases in plasma insulin, free fatty acids, triglycerides and total cholesterol. Liraglutide also attenuated hypoadiponectinemia-induced deterioration in peripheral and hepatic insulin sensitivity and alterations in key regulatory factors implicated in glucose and lipid metabolism. These findings demonstrated for the first time that liraglutide could be used to rescue IR induced by hypoadiponectinemia and HFD via regulating gene and protein expression involved in glucose and lipid metabolism.

© 2011 The Feinstein Institute for Medical Research, www.feinsteininstitute.org

Online address: <http://www.molmed.org>

doi: 10.2119/molmed.2011.00051

INTRODUCTION

Glucagonlike peptide (GLP)-1 is a 31-amino acid polypeptide hormone secreted by the L-cells of the gastrointestinal tract in response to a nutrient stimulus, which helps maintain glucose homeostasis through actions on α and β cells of the pancreas (1). Effects of GLP-1 include promoting glucose-mediated insulin secretion, lowering plasma glucagon, delaying gastric emptying and reducing appetite and food intake. In addition, it stimulates β -cell growth and proliferation (2–8), and insulin secretion in a glucose-dependent manner. The blood glucose-lowering effect of GLP-1, however, has been well demonstrated

(9,10); but native GLP-1 is not a viable therapeutic agent because it has a short half-life of <2 min, resulting from rapid degradation by the enzyme dipeptidyl peptidase IV (DPP-IV) and rapid renal elimination (11).

Liraglutide is a long-acting GLP-1 analog with a 97% sequence homology to human GLP-1. Functionally, it is similar to human GLP-1, but with structural modifications including an amino acid substitution of an arginine at position 34. There is also addition of a C-16 acyl chain linked to a glutamate spacer at the lysine on position 26 (12). These structural modifications result in reversible albumin binding, resistance to GLP-1 inactivation

by DPP-IV and prolonged duration of action (12). The physiological actions of liraglutide are mediated via specific GLP-1 receptors. Liraglutide shares several glucoregulatory actions with GLP-1, including enhancement of glucose-dependent insulin secretion, inhibition of postprandial glucagon secretion, inhibition of gastric emptying and reduction of food intake (13,14). In rodent studies, liraglutide promoted the maintenance of β -cell mass in diabetes, presumably by inhibiting both cytokine and free fatty acid (FFA)-induced apoptosis (15). Furthermore, clinical studies have found liraglutide to enhance β -cell function, suggesting a potential role in preservation of the β -cell (16). However, the physiological role of liraglutide in glucose and lipid metabolism and relevant signal transduction pathways still need to be determined. In previous studies, we have shown that exenatide, another GLP-1 analog, prevented fat-induced insulin resistance (IR) and

Address correspondence and reprint requests to Ling Li, Department of Clinical Biochemistry, Chongqing Medical University College of Laboratory Medicine, 400016 Chongqing, China. Phone: +86-23-68485216. Fax: +86-23-68486115; E-mail: lingli31@yahoo.com.cn.

Submitted February 6, 2011; Accepted for publication July 8, 2011; Epub (www.molmed.org) ahead of print July 11, 2011.

raised *adiponectin* (*Acrp30*) mRNA and protein levels (17). Thus, it will be of interest to determine whether liraglutide can regulate some genes involved in metabolic pathways.

Type 2 diabetes mellitus is commonly associated with IR, dyslipidemia and hypoadiponectinemia. To simulate the human conditions as closely as possible, we created a new mouse model where IR was produced by feeding a high-fat diet (HFD) to apolipoprotein (Apo)E^{-/-} mice that were dyslipidemic (19) and were made hypoadiponectinemic with recombinant adenovirus vectors expressing shRNA for *Acrp30* (Ad-shAcrp30). Furthermore, the effects of liraglutide administered twice daily for 8 wks on insulin sensitivity and gene expressions involved in gluco- and liporegulation were also investigated for this new mouse model. These results will lead to a more comprehensive understanding of the mechanisms of liraglutide's physiological actions on IR and provide new avenues for the therapeutic intervention of obesity and IR-related human disorders.

MATERIALS AND METHODS

Construction of shRNA-Expressing Adenoviruses

To construct adenoviral vectors expressing shRNA against *Acrp30*, we designed three short hairpin oligonucleotides and complementary strands to target specifically for mouse *Acrp30*. The AdEasy™ XL system (Stratagene, St. Clare, CA, USA) was used for shRNA construction. Briefly, the top and bottom oligonucleotides were annealed and ligated into the pSilencer1.0-U6 vector (Stratagene), and the sequence was confirmed. To evaluate the potency of these shRNAs *in vitro*, an *Acrp30* shRNA expression plasmid was transfected into the 3T3-L1 adipocyte line. Cells were harvested 48 h later for testing of knockdown efficiency. To generate the recombinant adenovirus vectors expressing shRNA for *Acrp30* (Ad-shAcrp30), pSilencer1.0-U6-shRNA plasmids were recombined into the Gateway-based pAd-AdEasy™ XL vector (Stratagene), accord-

ing to the manufacturer's instructions. As a negative control, a recombinant adenovirus vector expressing an shRNA directed against GFP was generated (Ad-shGFP). Amplification of recombinant adenovirus was performed according to the manufacturer's instructions (Stratagene) using HEK 293A cells. Large-scale amplification and purification of recombinant adenoviruses were performed using the ViraBind Adenovirus Purification Kit according to the manufacturer's instructions (Cell Biolabs Inc., San Diego, CA, USA) (18).

Animal Pretreatment

Sixty-four male ApoE^{-/-} mice weighing between 26 and 30 g were purchased from the Experimental Animal Center of Beijing University of Medical Sciences (Beijing, China). The mice were housed in individual cages in a temperature-controlled room with a 12-h light/dark cycle, where they had free access to standard mouse chow and water. After 3 d, the mice were fed an HFD from which 33% of calories were provided by carbohydrate, 13% by protein and 54% by fat for 16 wks. Then, mice were randomly divided into two groups for intravenous glucose tolerance tests (IVGTTs, n = 28) and a hyperinsulinemic-euglycemic clamp study (n = 36). Four days before the study, mice were anesthetized with an intraperitoneal injection of Ketamine (100 mg/kg; Nembutal Abbott Laboratories, Abbott Park, IL, USA). A catheter was inserted into the right internal jugular vein and extended to the level of the right atrium. Another catheter was advanced through the left carotid artery until its tip reached the aortic arch. The free ends of both catheters were attached to long segments of steel tubing and tunneled subcutaneously around the side of the neck to the back of the neck, where they were exteriorized through a skin incision and then securely anchored to the skin by a standard wounded clip. At the end of the procedure, catheters were flushed with 300 μ L isotonic saline containing heparin (20 U/mL) and ampicillin (5 mg/mL) and then filled with a

viscous solution of heparin (300 U/mL) and 80% polyvinyl pyrrolidone (PVP-10; Fisher Scientific, Pittsburgh, PA, USA) to prevent refluxing of blood into the catheter lumen. All procedures were approved by the Chongqing Medical University Animal Care and Use Committee.

IVGTTs

A total of 28 ApoE^{-/-} mice were randomly assigned to four groups. The first group (H group, n = 7) was given liraglutide (Novo Nordisk, Bagsvaerd, Denmark), 1 mg/kg in 100 μ L sterile saline twice daily. The second group (M group, n = 7) was given 0.5 mg/kg liraglutide. The third group (L group, n = 7) was given 0.1 mg/kg liraglutide. And the fourth group (NC group, n = 7) was given 100 μ L sterile saline. All injections were given intraperitoneally twice daily in a volume of 0.1 mL for 8 wks. The overnight-fasting mice were given intravenous glucose (1 g/kg body weight), and venous blood was collected before (time 0) and after injection at indicated times for the measurement of glucose (Glucometer Elite; Bayer) and insulin (Figure 1A).

Hyperinsulinemic-Euglycemic Clamp Study

A total of 36 HFD-fed ApoE^{-/-} mice were subdivided into four groups. One group was given 100 μ L (1×10^9 plaque-forming unit [PFU]) of Ad-shGFP (GF group, n = 6). The second group received 100 μ L Ad-shAcrp30 (ADI group, n = 10). The third group was given 100 μ L Ad-shAcrp30 and liraglutide (HEA group, n = 10), and the fourth group was given 100 μ L sterile saline (HF group, n = 10). All adenoviral injections were given in the tail vein at the end of 14th and 15th week of HFD feeding. The HEA group was given liraglutide 1 mg/kg intraperitoneally twice daily for 8 wks. After an overnight fast (12 h), the hyperinsulinemic-euglycemic clamp was performed in awake and unrestrained mice as described previously (19). Briefly, high-performance liquid chromatography (HPLC)-purified [3 H]glucose (Amersham, Los Angeles, CA, USA) was in-

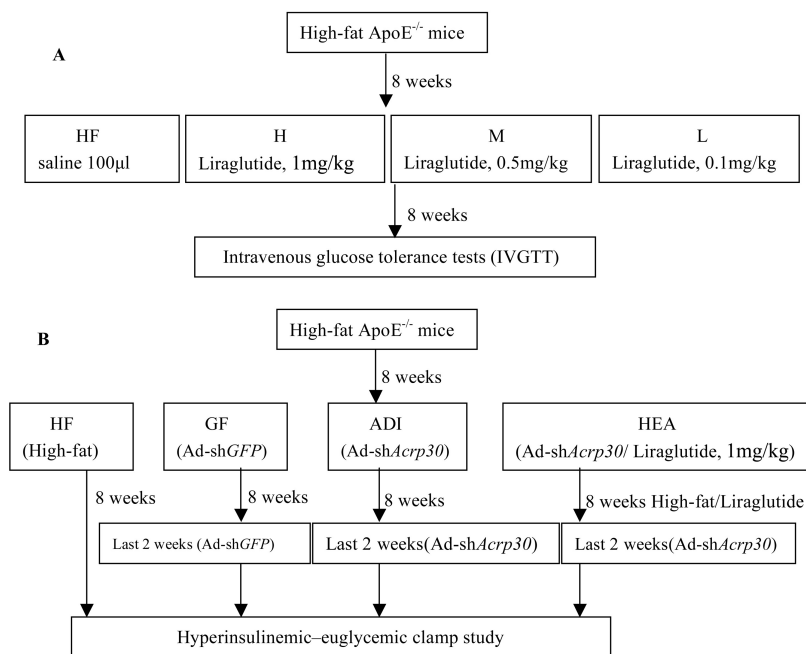


Figure 1. Experimental protocol. (A) IVGTT. (B) Hyperinsulinemic-euglycemic clamps.

fused through the carotid artery catheter starting at 0 min with a bolus ($5 \mu\text{Ci}$) followed by a continuous infusion ($0.05 \mu\text{Ci}/\text{min}$) for 90 min (basal period) to estimate the rate of basal glucose turnover. After the basal period, a 2-h hyperinsulinemic-euglycemic clamp was conducted with a primed, continuous infusion of human insulin ($5 \text{ mU} \cdot \text{kg}^{-1} \cdot \text{min}^{-1}$) to raise plasma insulin levels, whereas plasma glucose was maintained at a basal concentration with variable rates of 20% glucose infusion. Blood samples ($50 \mu\text{L}$) were taken at 80, 90, 100 and 120 min after the start of the clamps to determine plasma [$3\text{-}^3\text{H}$]glucose concentrations. Additional blood samples ($50 \mu\text{L}$) were collected before the start and at the end of the clamps process for measurement of plasma glucose, insulin, triglyceride (TG), total cholesterol (TC), low-density lipoprotein (LDL) cholesterol, high-density lipoprotein (HDL) cholesterol and FFA. During the clamp, each blood sample was replaced by the same volume of fresh whole blood from a donor mouse. At the end of the clamps, mice were anesthetized with a sodium pentobarbital injection. Within 5 min,

epididymal white adipose tissue and liver were collected. Each tissue, once exposed, was dissected out within 30 s, frozen immediately using liquid N_2 -cooled aluminum blocks and stored at -80°C for later analysis (Figure 1B).

Analytical Procedures

For the determination of plasma [$3\text{-}^3\text{H}$]glucose, plasma was deproteinized with ZnSO_4 and $\text{Ba}(\text{OH})_2$, dried to remove $3\text{H}_2\text{O}$, resuspended in water and counted in scintillation fluid (Ultima Gold; Packard Instrument, Meriden, CT, USA). Plasma FFA level was determined spectrophotometrically using an acyl-CoA oxidase-based colorimetric kit (Wako Pure Chemical Industries, Osaka, Japan). Plasma insulin concentrations were measured by radioimmunoassay using kits from Linco Research (St. Charles, MO, USA). Both plasma TG and TC concentrations were measured using enzymatic colorimetric methods (Sigma, St. Louis, MO, USA). Plasma Acrp30 was evaluated using a commercially available enzyme-linked immunosorbent assay (ELISA) kit (Phoenix Pharmaceuticals, Belmont, CA, USA).

Analysis of mRNA Expression by Real-Time Quantitative PCR

Total RNA was isolated from frozen liver or adipose tissue (approximately 85–100 mg) using Trizol reagent (Invitrogen, Carlsbad, CA, USA) according to the manufacturer's instructions. After treatment with DNase I (Invitrogen), purified RNA was used as template for first-strand cDNA synthesis using SuperScript III (Invitrogen). Quantitative real-time reverse transcriptase (RT)-PCR (QRT-PCR) was run using LC-Fast Start DNA SYBR Green I chemistry (Roche Diagnostics) on a LightCycler 2.0 platform (Roche Diagnostics). Gene expressions were analyzed using the comparative Ct method in relation to the levels of the β -actin. Forward and reverse primer pairs were as listed in Table 1.

Western Blot Analyses

Hepatic and adipose tissues were homogenized in 20 mmol/L 3-(*N*-morpholino)propanesulfonic acid (MOPS), 2 mmol/L ethylene glycol-bis(β -aminoethyl ether)-*N,N,N'*-tetraacetic acid (EGTA), 30 mmol/L sodium fluoride, 40 mmol/L β -glycerophosphate, 10 mmol/L sodium pyrophosphate, 2 mmol/L orthovanadate, 0.5% Tergitol-Type NP-40 (nonyl phenoxypolyethoxylethanol; Sigma-Aldrich, St. Louis, MO, USA) and complete phosphatase inhibitor cocktail (Roche Diagnostics). The protein concentration was measured with a BCA protein quantification kit (Pierce Biotechnology). One microliter of plasma and tissue extracts ($70 \mu\text{g}$) were separated by sodium dodecyl sulfate-polyacrylamide gel electrophoresis (12% resolving gel) and transferred to polyvinylidene fluoride membranes (Millipore) in a transfer buffer containing 20 mmol/L Tris, 150 mmol/L glycine and 20% methanol. Immunoblots were then blocked in Tris-buffered saline containing 0.1% Tween-20 (TBST) and 5% skim milk overnight at 4°C and incubated with primary antibody including Acrp30, phosphoenolpyruvate carboxykinase (PEPCK), hormone-sensitive lipase (HSL) and peroxisome proliferator-activated receptor (PPAR)- γ (Santa Cruz Biotechnol-

Table 1. Characteristics of the specific primers used for RT-PCR analysis.

Gene	Forward and reverse primers	Amplified fragment (bp)
<i>β-Actin</i>	5'-CCACTGCCGCATCCTCTTCCTC-3' 5'-TCCTGCTTGCTGATCCACATCT-3'	400
<i>GLUT-1</i>	5'-GAAACCCGCTGCTCATTG-3' 5'-TTGCTCCGTGTTCTGTG-3'	252
<i>GLUT-2</i>	5'-ACCCTGTTCTAACCAGGG-3' 5'-TGAACCAAGGGATTGGACC-3'	166
<i>GLUT-4</i>	5'-CTCTAATCCTGCCAGTCAT-3' 5'-GAGGCTCACCTTCACATCTTT-3'	395
<i>PEPCK</i>	5'-TCAACACCGACCTCCCTT-3' 5'-AGCATTGTGCCGCTATCT-3'	176
<i>PPARα</i>	5'-TACGGCAATGGCTTATCAC-3' 5'-CCCTCCTGCAACTTCTCAAT-3'	209
<i>PPARγ</i>	5'-GAAACCATGCGTGTATCCCT-3' 5'-AGACCACTCGCATTCCCTT-3'	266
<i>ATGL</i>	5'-TGCTACCCGCTGCTCTTTC-3' 5'-GACCTGATGACCACCCTTTC-3'	169
<i>HSL</i>	5'-GACTCACCGCTGACTTCC-3' 5'-TGTCTCGTTGCGTTTGTAG-3'	161
<i>HMGCR</i>	5'-TGGCAGGACGCAACCTCTAT-3' 5'-TGACGGCTTCACAAACCACA-3'	222
<i>LDLr</i>	5'-GAACTCAGGGCCTCTGTCTG-3' 5'-GAAACCATGCGTGTATCCCT-3'	188
<i>ACC</i>	5'-CTGTGAGGTGGATCAGAGAT-3' 5'-TTCAGCTCTAACTGGAAGC-3'	129
<i>FAS</i>	5'-TGGTGGGTTGGTGAATTGTC-3' 5'-GCTTGTCTGCTCTAACTGGAAGT-3'	213
<i>SCD1</i>	5'-CTACAAGCCTGGCCTCCTGC-3' 5'-GGACCCCAGGGAAACCAGGA-3'	226
<i>INSIG-1</i>	5'-ATCACGCCAGTGCTAAAGTA-3' 5'-CAACCAAGAACGGACATAGA-3'	410
<i>INSIG-2</i>	5'-ATCACGCCAGTGCTAAAGTA-3' 5'-CAACCAAGAACGGACATAGA-3'	221
<i>SREBP-1</i>	5'-TGGAGA CATCGCAAACAAG-3' 5'-GGTAGACAACAGCCGCATC-3'	274
<i>SREBP-2</i>	5'-CTGGTACGCTGGTACTCAA-3' 5'-GCTGTCAGGTGGATCTCAAT-3'	263

ogy, Santa Cruz, CA, USA) (1:200 dilution) and β -Actin (Research Diagnostics) (1:500 dilution) for 2 h at room temperature. After three consecutive 5-min washes in TBST, blots were incubated with horseradish peroxidase-conjugated secondary antibody (Invitrogen) (1:500 dilution with TBST) for 1 h at room temperature. After two washes in TBST and a final wash in Tris-buffered saline, the blots were scanned using the Odyssey Infrared Imaging System (LI-COR Biosciences), and quantification of antigen-antibody complexes was performed using Quantity One analysis software (Bio-Rad).

Calculations

Glucose rates of appearance (GRa) were determined with $3\text{-}[^3\text{H}]\text{glucose}$ as described. GRa and whole-body glucose uptake (glucose disposal rate [GRd]) were calculated using the non-steady-state equation of Steele *et al.* (20). The distribution volume for glucose was assumed to be 150 g/kg. Hepatic glucose production (HGP) was calculated as the difference between the isotopically determined GRa and the rate of glucose infused to maintain euglycemia (glucose infusion rate [GIR]): $\text{HGP} = \text{GRa} - \text{GIR}$.

Statistical Analysis

Data are presented as means \pm SD. A repeated-measures analysis of variance was used to assess the results measured at consecutive multiple time points. A two-way design was used to incorporate additional effects of different experimental groups followed by a *post hoc* protected least significant difference (PLSD) test to compare two individual groups. Differences were statistically significant at $P < 0.05$. All analyses were performed using SPSS (SPSS graduate pack; SPSS, Chicago, IL, USA).

RESULTS

Adiponectin Gene Silencing

A previously validated shRNA sequence against *Acrp30* was engineered into an adenovirus vector (Ad-shAcrp30) and tested for relative silencing efficiency compared with a control sequence (Ad-shGFP) (18). Treatment with Ad-shAcrp30 achieved a 76% reduction of *Acrp30* expression in adipose tissues (Figure 2A) and a 35% reduction of plasma Acrp 30 level in the ADI group than in HEA, HF or GF groups (6.07 ± 2.17 versus 9.67 ± 2.05 , 9.53 ± 2.50 and 9.14 ± 2.87 $\mu\text{g/L}$, respectively; $P < 0.01$; Figure 2B). As expected, Ad-shAcrp30 treatment in ADI mice significantly decreased Acrp30 protein levels in adipose tissues (a 48.3% reduction opposed to the HF group; Figure 2C), whereas liraglutide treatment prevented the reduction of Acrp30.

Basal Metabolic Parameters

Fasting plasma insulin, FFAs, TGs and TC were significantly increased in the ADI group (all $P < 0.01$, Table 2). Liraglutide treatment significantly decreased body weight and fasting blood glucose compared with the other three groups (all $P < 0.01$, see Table 2).

Effect of Liraglutide on IVGTT

The peak glucose levels achieved over the first 10 min of the IVGTT were significantly lower in the H group than in the L, M and NC groups. Plasma glucose

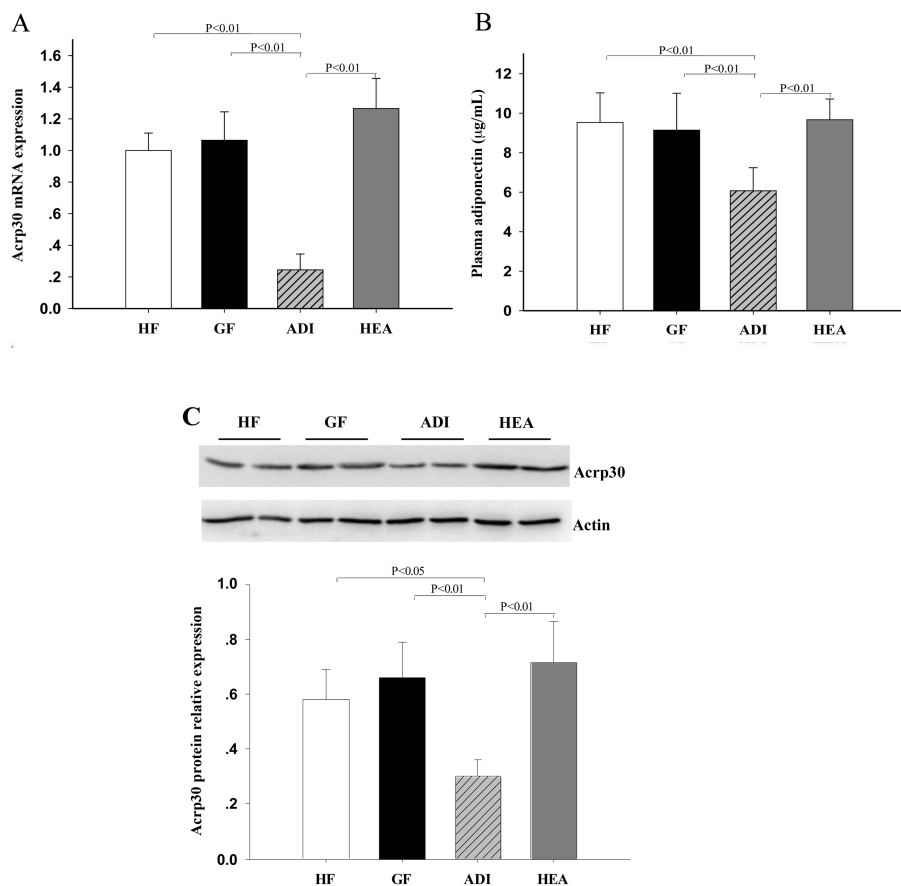


Figure 2. Acrp30 knockdown in HFD-fed ApoE^{-/-} mice. Mice were injected with adenoviruses expressing either shGFP or shAcrp30. A subgroup of the mice was injected with liraglutide at a dose of 1 mg/kg twice daily. (A) Relative *Acrp30* mRNA levels in adipose tissues. (B) Plasma Acrp30 levels. (C) Acrp30 protein levels in adipose tissues.

levels returned to baseline within 30 min in the H groups, whereas the return to baseline was delayed in the M, L and NC groups (Figures 3A–E). Insulin responses to intravenous glucose were significantly increased in the H group compared with the L and HF groups, with intermediate values in the M group (Figures 3F–J).

Effects of Liraglutide on Glucose and Lipid Metabolism during the Hyperinsulinemic-Euglycemic Clamp

Hyperinsulinemic-euglycemic clamps were performed approximately 24 h after the last liraglutide treatment and after an overnight fast. Plasma glucose was clamped at approximately 5.8 mmol/L in all groups. Plasma insulin concentrations were raised to approximately four to five

times basal values. Despite identical insulin infusion rates ($5 \text{ mU} \cdot \text{kg}^{-1} \cdot \text{min}^{-1}$), plasma insulin levels were higher in the

ADI group than in the HF, GF and HEA groups ($P < 0.01$, Table 3). Plasma FFAs, TC and TGs were significantly suppressed during the clamp procedures in four groups, but remained higher in the ADI group than in the other three groups (all $P < 0.01$, see Table 3). As expected, the ADI group required a much lower GIR than the HF and GF mice did during the clamp procedure. Surprisingly, liraglutide treatment markedly increased the GIR in the HEA mice to levels similar to those observed in HF or GF mice (see Table 2). Similarly, isotopically determined insulin-stimulated GRd was lower in the ADI group than in the HF and GF groups ($P < 0.01$, see Table 3). In addition, the ability of insulin to suppress HGP during clamps was significantly impaired in the ADI group compared with the HF and GF groups ($P < 0.01$, see Table 3). However, liraglutide treatment also prevented these changes (see Table 3).

Effects of Liraglutide on Genes Involved in Glucose Metabolism

To assess the effects of liraglutide on gene expression involved in glucose metabolism in ApoE^{-/-} mice with hypoadiponectinemia, we used QRT-PCR analyses to examine *PEPCK*, *glucose transporter-1 (GLUT-1)*, *GLUT-2* and *GLUT-4* mRNA expression in the liver. Hepatic *PEPCK* mRNA expression was significantly upregulated (~58%), whereas *GLUT-1* mRNA expression was significantly downregulated (~63%) in

Table 2. Basal metabolic characteristics.

Index	HEA	HF	GF	ADI
n	6	6	6	6
Body weight (g)	26.7 ± 0.9	29.4 ± 1.3 ^a	28.5 ± 1.2 ^a	28.9 ± 1.4 ^a
Fasting blood glucose (mmol/L)	7.0 ± 0.4	7.7 ± 0.8 ^a	7.7 ± 0.4 ^a	7.9 ± 0.7 ^a
FFA (mmol/L)	3.11 ± 0.22 ^b	3.10 ± 0.09 ^b	3.10 ± 0.10 ^b	3.60 ± 0.18
TG (mmol/L)	2.2 ± 0.1 ^b	2.3 ± 0.2 ^b	2.2 ± 0.2 ^b	2.7 ± 0.3
TC (mmol/L)	21.1 ± 0.4 ^b	21.9 ± 1.8 ^b	20.9 ± 2.4 ^b	24.5 ± 3.1
HDL cholesterol (mmol/L)	4.6 ± 0.5 ^b	4.6 ± 0.8 ^b	4.5 ± 0.5 ^b	3.8 ± 0.4
LDL cholesterol (mmol/L)	13.6 ± 2.3 ^b	14.0 ± 2.1 ^c	13.7 ± 2.2 ^b	16.9 ± 2.1
Insulin (mU/L)	111.3 ± 12.8 ^b	111.1 ± 13.0 ^b	112.1 ± 13.6 ^b	127.9 ± 11.2

Data are means ± SE.

^a $P < 0.01$ versus the HEA group.

^b $P < 0.01$, ^c $P < 0.05$, versus the ADI group.

Effects of Liraglutide on Genes Involved in Triglyceride Metabolism

To investigate the impact of liraglutide on gene expressions involved in TG metabolism in hypoadiponectinemia and diet-induced insulin-resistant ApoE^{-/-} mice, we next examined the *PPAR γ* , *adipose triglyceride lipase (ATGL)* and *HSL* mRNA expressions of adipose tissues by QRT-PCR. The mRNA expressions of *HSL* and *PPAR γ* in adipose tissues were significantly downregulated in the ADI group (~31% and ~44%, both $P < 0.01$; Figures 5A, B). Mirroring the changes in gene expression, Western blot analyses revealed that both *HSL* and *PPAR γ* protein levels were similarly decreased (60.3% and 65.4% reduction opposed to the HF group, both $P < 0.01$; Figure 5F). However, liraglutide treatment prevented these changes (Figures 5A, B and F). *ATGL* and *sterol regulatory element binding protein (SREBP)-1* mRNA levels were not different among the four groups (data not shown).

Effects of Liraglutide on Gene Expression Involved in Fatty Acid Metabolism

To examine whether liraglutide plays a role in fatty acid metabolism of adipose tissues in the development of IR in ApoE^{-/-} mice induced by hypoadiponectinemia and HFD, the mRNA expressions of *acetyl-CoA carboxylase (ACC)*, *fatty acid synthetase (FAS)* and *stearoyl-CoA desaturase-1 (SCD-1)* in adipose tissue were examined. The administration of Ad-shAcrp30 significantly upregulated the *FAS* mRNA expression of adipose tissue (~1.8-fold, $P < 0.01$, Figure 5C). However, treatment of liraglutide restored it (Figure 5C) and downregulated *ACC* (~58%, Figure 5D) and *SCD1* mRNA expressions (~83%, $P < 0.01$, Figure 5E).

Effects of Liraglutide on Gene Expressions Involved in Cholesterol Metabolism

Hypercholesteremia in ApoE^{-/-} mice with hypoadiponectinemia indicated that cholesterol metabolic disorder

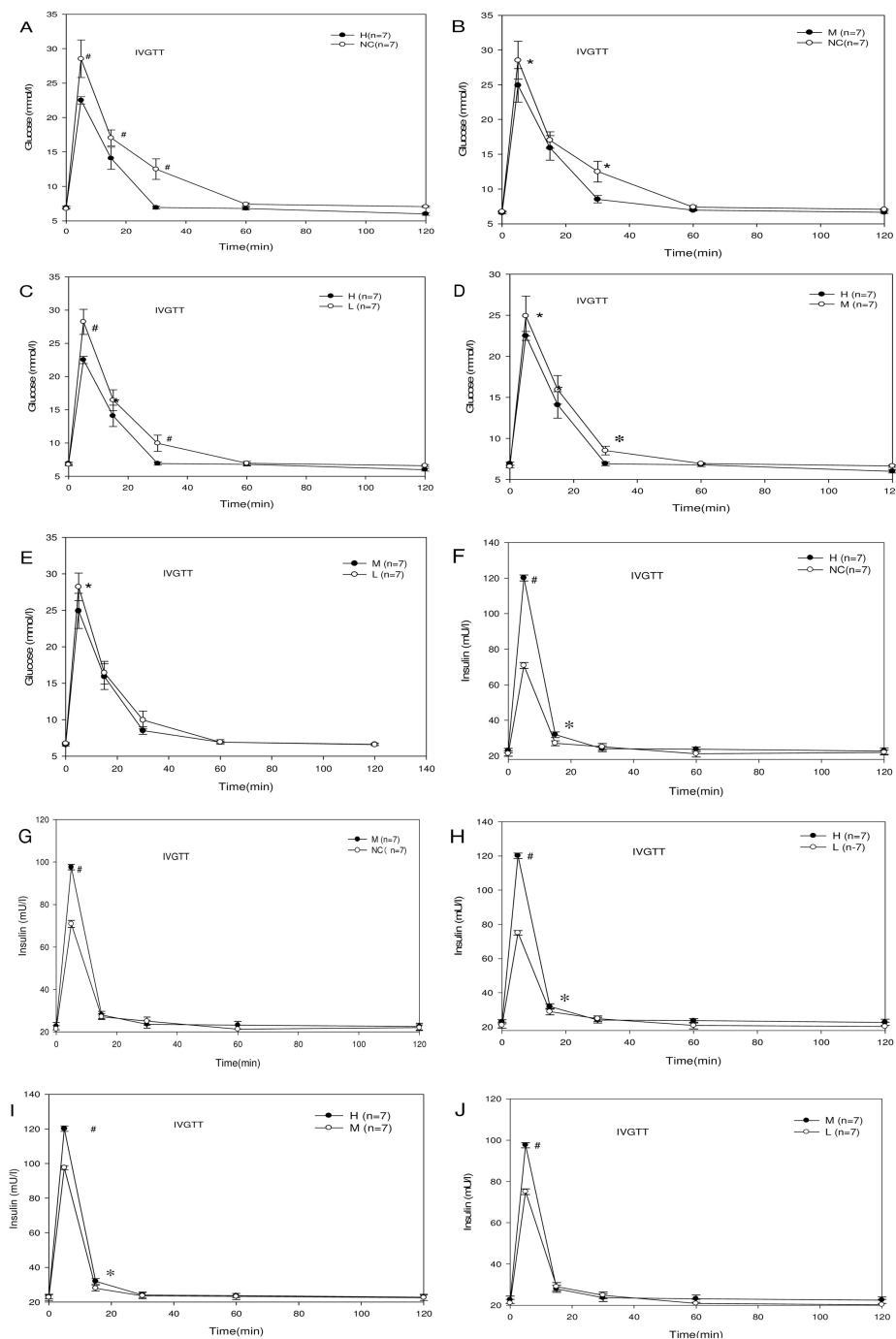


Figure 3. IVGTT. (A-E) Glucose curves in four groups. (F-J) Insulin curves in four groups. Values are presented as means \pm SE; * $P < 0.05$, # $P < 0.01$.

the ADI group opposed to the other three groups ($P < 0.05$ and $P < 0.01$; Figures 4A, B). Consistent with *PEPCK* mRNA expression, hepatic *PEPCK* protein was markedly increased in the ADI

group compared with the other groups (Figure 4C). However, hepatic *GLUT-2* and *GLUT-4* mRNA expression remained unchanged in four groups (data not shown).

Table 3. Plasma parameters and glucose turnover data in four groups during the insulin clamp.

Index	HEA (n = 10)		HF (n = 10)		GF (n = 6)		ADI (n = 10)	
	Basal	Clamp	Basal	Clamp	Basal	Clamp	Basal	Clamp
Fasting blood glucose (mmol/L)	7.0 ± 0.4	5.8 ± 0.1	7.7 ± 0.8 ^a	5.8 ± 0.2	7.7 ± 0.4 ^a	5.8 ± 0.1	7.9 ± 0.7 ^a	5.8 ± 0.2
Insulin (mU/L)	111.3 ± 12.8 ^b	415.0 ± 14.6 ^{b,c}	111.1 ± 13.0 ^b	408.6 ± 10.5 ^{b,c}	112.1 ± 13.6 ^b	411.2 ± 12.6 ^{b,c}	127.9 ± 11.2	490.7 ± 13.9 ^c
TC (mmol/L)	21.1 ± 0.4 ^b	13.8 ± 2.4 ^{b,c}	21.9 ± 1.8 ^b	13.7 ± 2.4 ^{b,c}	20.9 ± 2.4 ^b	14.0 ± 2.5 ^{b,c}	24.5 ± 3.1	17.2 ± 1.9 ^c
TG (mmol/L)	2.22 ± 0.14 ^b	1.31 ± 0.29 ^{b,c}	2.28 ± 0.18 ^b	1.32 ± 0.10 ^{b,c}	2.23 ± 0.20 ^b	1.30 ± 0.12 ^{b,c}	2.70 ± 0.32	2.14 ± 0.18 ^c
FFA (mmol/L)	3.11 ± 0.22 ^b	1.64 ± 0.45 ^{b,c}	3.10 ± 0.09 ^b	1.66 ± 0.22 ^{b,c}	3.11 ± 0.10 ^b	1.60 ± 0.22 ^{b,c}	3.55 ± 0.18	2.21 ± 0.25 ^c
GIR (mg · kg ⁻¹ · min ⁻¹)	—	30.9 ± 2.4 ^b	—	30.2 ± 3.1 ^b	—	31.1 ± 2.3 ^b	—	21.8 ± 3.6
GRd (mg · kg ⁻¹ · min ⁻¹)	16.4 ± 0.3 ^d	38.1 ± 0.7 ^{b,c}	16.2 ± 0.3 ^b	38.2 ± 0.8 ^{b,c}	16.0 ± 0.6 ^b	38.6 ± 1.1 ^{b,c}	17.0 ± 0.6	35.8 ± 1.1 ^c
HGP (mg · kg ⁻¹ · min ⁻¹)	16.4 ± 0.3 ^d	7.2 ± 2.3 ^{b,c}	16.2 ± 0.3 ^b	8.0 ± 5.5 ^{b,c}	16.0 ± 0.6 ^b	6.8 ± 2.2 ^{b,c}	17.0 ± 0.6	14.4 ± 2.7 ^c

Data are means ± SE. ADI, high-fat fed mice treated with pAd-U6- Acrp30; HEA, high-fat fed mice treated with pAd-U6-Acrp30 and liraglutide at a dose of 1 mg/kg once daily; HF, HFD-fed mice treated with saline; GF, HFD-fed mice treated with pAd-U6-GFP

^a*P* < 0.01 versus HEA group.

^b*P* < 0.01, ^d*P* < 0.05, versus the ADI group.

^c*P* < 0.01 versus basal values.

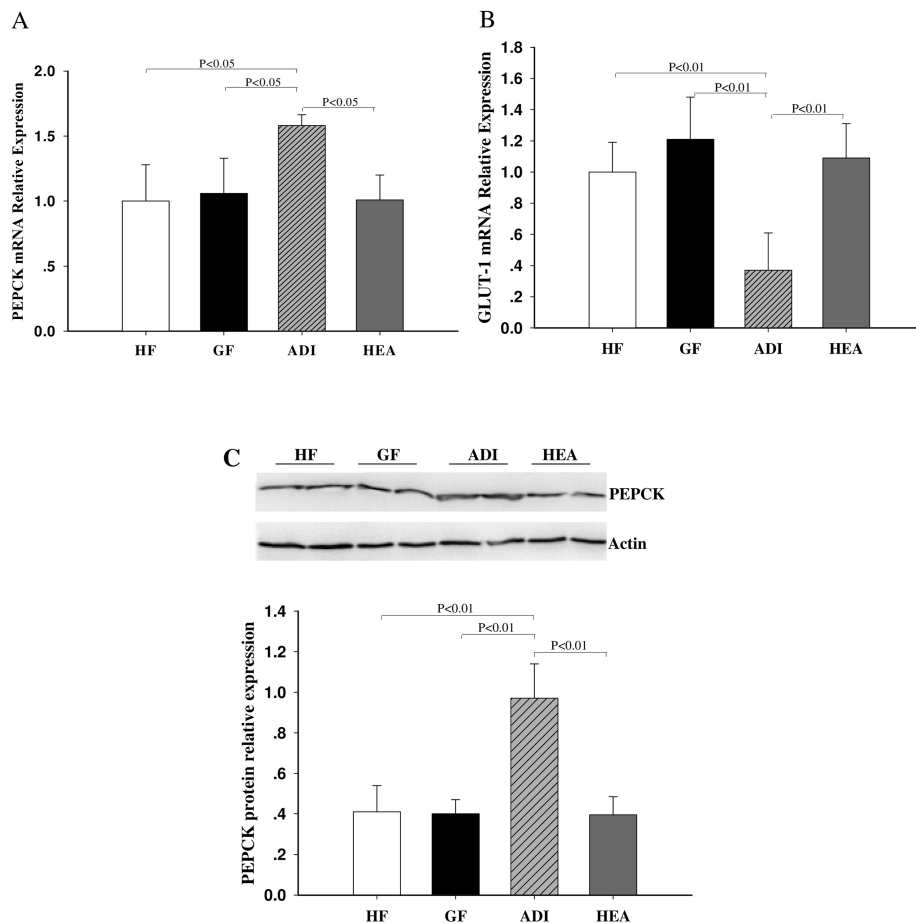


Figure 4. Real-time RT-PCR and Western immunoblot analysis of hepatic *PEPCK* and *GLUT-1*. (A) *PEPCK* mRNA expression. (B) *GLUT-1* mRNA expression. (C) *PEPCK* protein level graphs show the averages ± SD for each parameter obtained (n = 6 mice per group).

might play an important role in the development of IR. To investigate the potential mechanisms responsible for cholesterol metabolic disorder, we next examined the expressions of *insulin-induced gene (INSIG)-1* and *INSIG-2*, *SREBP-2*, *3-hydroxy-3-methylglutaryl coenzyme A reductase (HMGCR)*, *PPARα* and *LDL receptor (LDLr)* in the liver. The administration of Ad-shAcrp30 significantly downregulated the mRNA expression of *INSIG-2* (~70%, *P* < 0.01), *LDLr* (~45%, *P* < 0.01) and *PPARα* (~43%, *P* < 0.01) in liver of ApoE^{-/-} mice. Treatment of liraglutide restored the mRNA expression of *INSIG-2*, *LDLr* and *PPARα* (Figures 6A, C and D) and further upregulated *HMGCR* and *SREBP-2* mRNA expression (~49%, *P* < 0.05, and ~89%, *P* < 0.01; Figures 6B, E).

DISCUSSION

On a chow diet, the ApoE^{-/-} mouse developed mild but significant hypercholesterolemia with elevated LDL cholesterol levels. The fasting glucose and insulin levels on this diet remained in the normal range. Our previous study demonstrated that ApoE^{-/-} mice fed an HFD developed more severe hypercholesterolemia, markedly elevated LDL cholesterol levels and modest increased TG, fasting blood glucose and body weight, suggesting severe IR (21). Then, we reported that exenatide, another

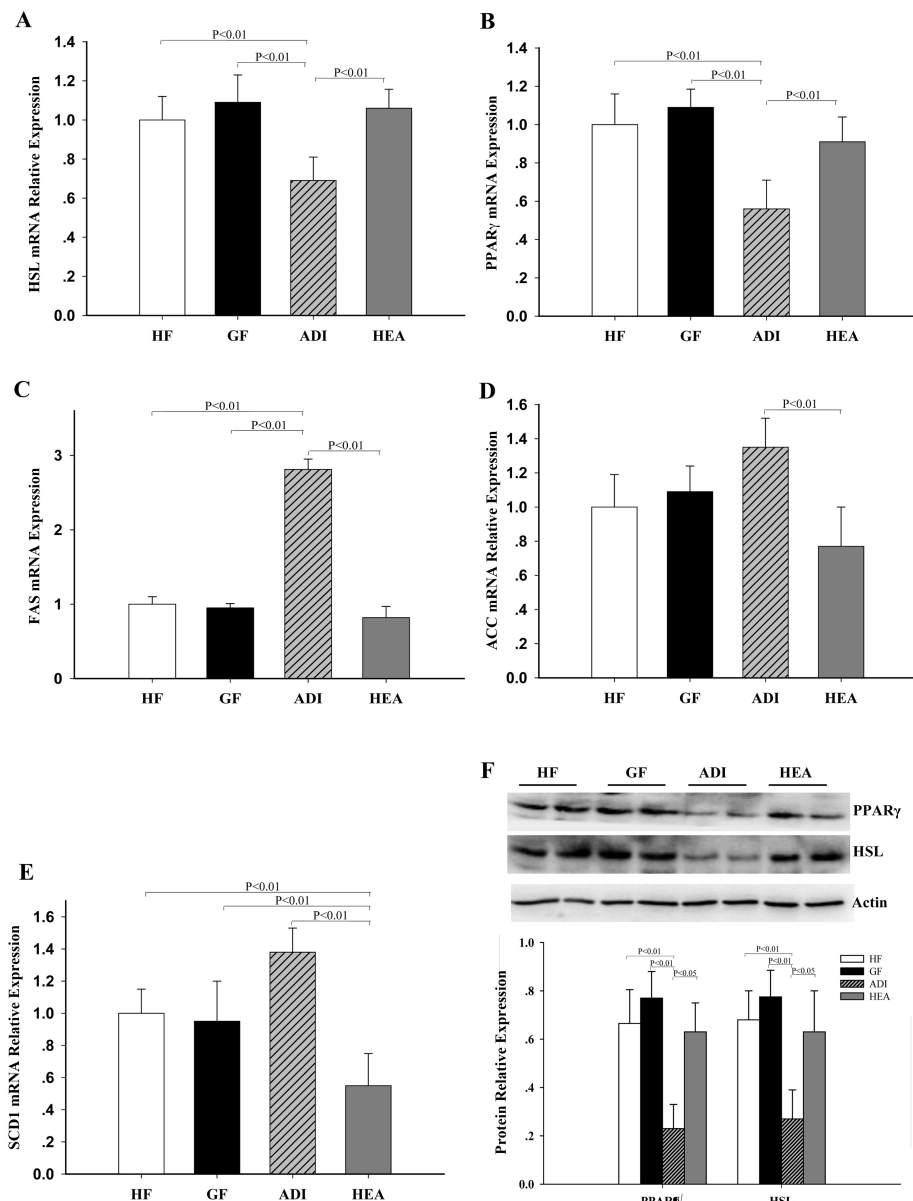


Figure 5. Effects of liraglutide on gene expression involved in TG and fatty acid metabolism in adipose tissues. (A) *HSL* mRNA expression. (B) *PPAR γ* mRNA expression. (C) *FAS* mRNA expression. (D) *ACC* mRNA expression. (E) *SCD1* mRNA expression. (F) *PPAR γ* and *HSL* protein levels. Graphs show the average \pm SEM for each parameter obtained ($n = 6$ mice per group).

GLP-1 analog, prevented fat-induced IR and raised *Acrp30* mRNA and protein levels (17). In *in vitro* study, we also confirmed that the transfection of Ad-shAcrp30 significantly decreased *Acrp30* mRNA expression and its protein level in 3T3-L1 adipocytes. The *Acrp30* knock-down also markedly reduced the cellular

glucose uptake rate, increased intracellular TG content and downregulated the mRNA expression of insulin receptor substrate-1 in both basal and insulin-stimulated states in the transfected cells (18). The present report demonstrated that the use of Ad-shAcrp30 can result in a higher silencing efficiency, that both

Acrp30 mRNA and *Acrp30* protein expression was significantly reduced by 76% and 48.3% in adipose tissues and that plasma *Acrp30* level was also reduced by 37%, which allowed us to evaluate the metabolic impact and underlying mechanisms of knocking down *Acrp30* in an IR model. In ApoE^{-/-} mice fed an HFD, the administration of Ad-shAcrp30 developed mild but significant hyperinsulinemia, elevated plasma glucose and FFAs, markedly decreased plasma *Acrp30* and HDL cholesterol and further increased TG, TC and LDL cholesterol. Thus, in ApoE^{-/-} mice, HFD and Ad-shAcrp30 treatment promoted the development of features of IR, including obesity, hyperglycemia, hyperinsulinemia and elevating FFAs.

To examine the impact of *Acrp30* deficiency on diet-induced IR, we next performed an insulin clamp study in ApoE^{-/-} mice. Indeed, the chronic deficiency of *Acrp30* further led to a decrease in GIR and insulin's ability to suppress HGP. These decreases were accompanied by a dramatic reduction of *GLUT-1* and an increase of both *PEPCK* mRNA and protein expression in the liver. *GLUT-1* is thought to be involved in glucose transport in the basal metabolic state. The reduction of *GLUT-1* markedly decreased basal glucose transport and caused impairment of insulin stimulation of transport (22). A defect in glucose transport is responsible for the IR in type 2 diabetes (23). *PEPCK* is a key enzyme of HGP. It has been shown, when overexpressed, to induce IR *in vivo* and disturb both glucose and lipid homeostasis (24). Thus, the increase in glucose production in ADI mice was accounted for by a marked promotion of gluconeogenesis via increasing hepatic *PEPCK* mRNA and protein levels. These results entirely accounted for the effects of *Acrp30* deficiency on glucose metabolism and insulin action. Importantly, in HFD apoE^{-/-} mice treated with both Ad-shAcrp30 and liraglutide, *PEPCK* mRNA and protein levels were markedly suppressed, whereas *GLUT-1* mRNA expression was elevated to levels similar to those of HFD apoE^{-/-} mice. A

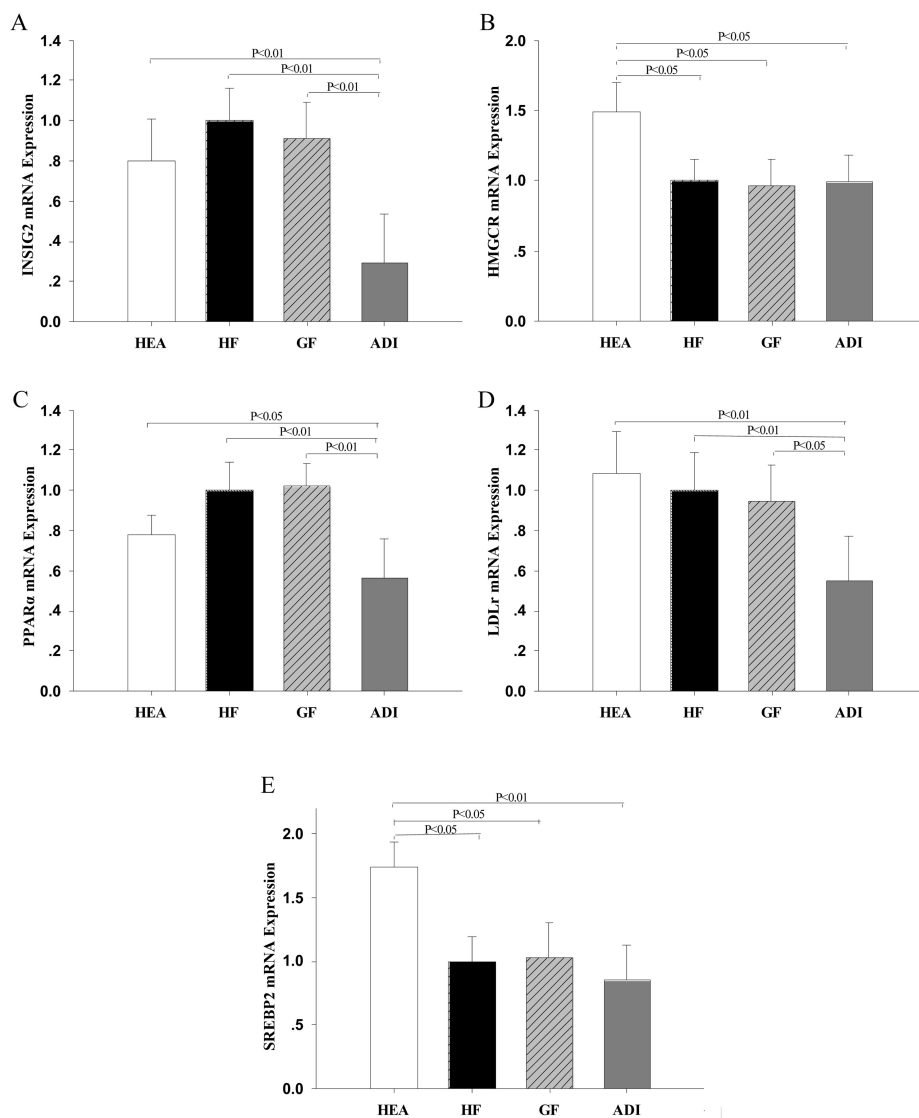


Figure 6. Effects of liraglutide on gene expression involved in cholesterol metabolism in liver. (A) *INSIG-2* mRNA expression. (B) *HMGCR* mRNA expression. (C) *PPAR α* mRNA expression. (D) *LDLr* mRNA expression. (E) *SREBP-2* mRNA expression.

reduction in *PEPCK* activity in liver probably resulted in the inhibitory effect of liraglutide on hepatic gluconeogenesis. Therefore, increases in the GIR and inhibition in HGP accounted for the ameliorating IR in liraglutide-treated mice.

In this study, we also demonstrated that the mRNA and protein expressions of *HSL* and *PPAR γ* in adipose tissue were significantly downregulated in *ApoE*^{-/-} mice with hypoadiponectinemia. However, liraglutide intervention markedly increased the mRNA and protein expres-

sions of *HSL* and *PPAR γ* to levels similar to those observed in mice only fed an HFD. The primary action attributed to *HSL* is hydrolysis of stored TG in adipose tissue (that is, lipolysis). Indirect evidence has suggested that *HSL* is the rate-limiting enzyme in intracellular lipolysis (25). Therefore, it is possible that a reduction of *HSL* mRNA and protein expression in *ApoE*^{-/-} mice with *Acrp30* deficiency could promote adipose tissue to accumulate TG and decrease releasing FFAs, thereby providing a com-

pensatory mechanism for the elevated FFA level and IR.

PPAR γ is known to play a key role in adipogenesis and appears to be a master controller of the “thrifty gene response” that leads to efficient energy storage in adipocytes (26). It regulates expressions of a number of genes involved in lipid metabolism, including *HSL* and *lipoprotein lipase (LPL)*. *PPAR γ* activation also efficaciously ameliorates whole-body and muscle IR and hypertriglyceridemia (27). Here we found that Ad-shAcrp30 treatment greatly diminished both *PPAR γ* mRNA and protein expressions in *ApoE*^{-/-} mice. This diminishing was accompanied by elevated plasma FFAs; further increased TG, TC and LDL cholesterol; and a parallel low GIR and rate of HGP inhibition during the hyperinsulinemic-euglycemic clamp, further addressing the important role of *PPAR γ* in the regulation of insulin sensitivity and TG homeostasis in these animals. Thus, the effects of *Acrp30* deficiency on insulin signaling, glucose fluxes and lipid homeostasis are, at least in part, due to the suppression of the *PPAR γ* pathway. Of interest, treatment of *ApoE*^{-/-} mice with liraglutide prevented the decrease of *PPAR γ* and *HSL* mRNA and protein expressions, which demonstrated the TG homeostasis and insulin-sensitizing action of liraglutide via the marked activation of this pathway.

In this study, we also showed that hepatic *PPAR α* mRNA levels in mice with hypoadiponectinemia were significantly downregulated compared with those fed only an HFD. However, liraglutide treatment reversed this effect, at least in part, reducing hepatic *PPAR α* expression induced by hypoadiponectinemia. *PPAR α* is a ligand-activated transcriptional factor that plays an important role in lipid metabolism. It regulates a number of genes involved in cholesterol homeostasis, plasma lipoproteins and glucose levels (28,29). Our results suggested that hypoadiponectinemia induced a decreased *PPAR α* activity. Therefore, changes in *PPAR α* activity accompanied with the alteration of plasma cholesterol accounts

for, at least in part, cholesterol metabolic disturbance in mice with hypoadiponectinemia. This concept was further supported by our finding of lowered hepatic *LDLr* mRNA expression, which may function in the removal of the LDL cholesterol particles from circulation by the liver, in mice with hypoadiponectinemia, whereas lowered *LDLr* mRNA was also prevented by liraglutide administration.

In the liver, hypoadiponectinemia also led to the reduction of *INSIG-2* mRNA, which has shown the potential to block cholesterol and fatty acid synthesis and has been implicated as a susceptibility gene for plasma cholesterol levels in mice (30). However, liraglutide administration restored the alteration of *INSIG-2* transcript level and elevated the *SREBP-2* transcript. *SREBP-2* preferentially activates the *LDLr* gene and various genes required for cholesterol synthesis, such as HMG-CoA reductase (31). *INSIG-2* is a polytopic endoplasmic reticulum (ER) membrane protein that reduces cholesterol synthesis by blocking the translocation of the *SREBP cleavage-activating protein (SCAP)* complex and the proteolytic activation of *SREBP*. Thus, when hypoadiponectinemia, lower *INSIG-2* transcript level facilitated the translocation of the *SCAP* complex from ER to Golgi and the proteolytic activation of *SREBP* (32,33). Hence, hepatic cholesterol synthesis was increased and resulted in an elevated plasma cholesterol level. After liraglutide administration, the increase in *INSIG-2* transcript level prevented the translocation of the *SCAP* complex and the activation of *SREBP*. As a result, the synthesis of cholesterol was inhibited and the plasma cholesterol level declined. However, the finding that gene expression of *SREBP-2* increased in mice treated with liraglutide might have been due at least in part to the fact that liraglutide initially caused a reduction of cholesterol synthesis and plasma cholesterol levels, leading to a feedback mechanism that might then cause an upregulation of *SREBP-2*.

In adipose tissues, the most prominently affected genes were *ACC*, *FAS* and

SCD1, which were key lipogenic genes involved in lipid metabolism (34). Hypoadiponectinemia led to a substantial increase in mRNAs encoding *FAS*. This result suggested a substantial net increase of *de novo* lipogenesis in adipose tissues coupled with increasing body weight and IR in mice with hypoadiponectinemia. Importantly, the treatment of liraglutid prevented the increase of *FAS* transcript level led by hypoadiponectinemia and further decreased *ACC* and *SCD1* transcript levels compared with mice with hypoadiponectinemia. These data further suggested that changes in transcript levels of *FAS*, *ACC* and *SCD1* contributed to the antiobesity and IR efficacy of liraglutid.

In conclusion, this study was the first to reveal the profound anti-IR effect of liraglutid when administered systemically in murine models of hypoadiponectinemia and HFD. Our data clearly indicated that the effects of liraglutid were, at least in part, likely mediated by the alterations of gene and protein expressions involved in glucose and lipid metabolism, especially *Acrp30*. Taken together, these results suggest that liraglutid might prevent the earliest stage of diet- and hypoadiponectinemia-induced IR and lead to a novel strategy for preventing the development of IR and diabetes.

ACKNOWLEDGMENTS

This work was supported by grants from the National Natural Science Foundation of China (30871199, 30771037, 30971388 and 81070640) and the Doctoral Fund of Ministry of Education of China (20105503110002).

DISCLOSURE

The authors declare that they have no competing interests as defined by *Molecular Medicine*, or other interests that might be perceived to influence the results and discussion reported in this paper.

REFERENCES

1. Kieffer TJ, Habener JF. (1999) The glucagon-like peptides. *Endocr. Rev.* 20:876–913.

2. Agero H, Vicini P. (2003) Pharmacodynamics of NN2211, a novel long acting GLP-1 derivative. *Eur. J. Pharm. Sci.* 19:141–50.
3. Holst JJ, Orskov C, Nielsen OV, Schwartz TW. (1987) Truncated glucagon-like peptide I, an insulin-releasing hormone from the distal gut. *FEBS Lett.* 211:169–74.
4. Kreymann B, Williams G, Ghatei MA, Bloom SR. (1987) Glucagonlike peptide-1 7–36: a physiological incretin in man. *Lancet.* 2:1300–4.
5. Wettergren A, et al. (1993) Truncated GLP-1 (proglucagon 78-107-amide) inhibits gastric and pancreatic functions in man. *Dig. Dis. Sci.* 38:665–73.
6. Naslund E, et al. (1999) Energy intake and appetite are suppressed by glucagon-like peptide-1 (GLP-1) in obese men. *Int. J. Obes. Relat. Metab. Disord.* 23:304–11.
7. Naslund E, et al. (1999) GLP-1 slows solid gastric emptying and inhibits insulin, glucagon, and PYY release in humans. *Am. J. Physiol. Regul. Integr. Comp. Physiol.* 277:R910–16.
8. Edvell A, Lindstrom P. (1999) Initiation of increased pancreatic islet growth in young normoglycemic mice (Umea +/-). *Endocrinology.* 140:778–83.
9. Willms B, et al. (1996) Gastric emptying, glucose responses, and insulin secretion after a liquid test meal: effects of exogenous glucagon-like peptide-1 (GLP-1)-(7-36) amide in type 2 (noninsulindependent) diabetic patients. *J. Clin. Endocrinol. Metab.* 81:327–32.
10. Rachman J, Barrow BA, Levy JC, Turner RC. (1997) Nearnormalisation of diurnal glucose concentrations by continuous administration of glucagon-like peptide-1 (GLP-1) in subjects with NIDDM. *Diabetologia.* 40:205–11.
11. Meier JJ, et al. (2004) Secretion, degradation, and elimination of glucagon-like peptide 1 and gastric inhibitory polypeptide in patients with chronic renal insufficiency and healthy control subjects. *Diabetes.* 53:654–62.
12. Knudsen LB, et al. (2000) Potent derivatives of glucagon-like peptide-1 with pharmacokinetic properties suitable for once daily administration. *J. Med. Chem.* 43:1664–9.
13. Naslund E, Gutniak M, Skogar S, Rossner S, Hellstrom PM. (1998) Glucagon-like peptide 1 increases the period of postprandial satiety and slows gastric emptying in obese men. *Am. J. Clin. Nutr.* 68:525–30.
14. Bregenholt S, et al. (2005) The long-acting glucagonlike peptide-1 analogue, liraglutide, inhibits beta-cell apoptosis in vitro. *Biochem. Biophys. Res. Commun.* 330:577–84.
15. Mari A, et al. (2007) Effects of the long-acting human glucagon-like peptide-1 analog liraglutide on beta-cell function in normal living conditions. *Diabetes Care.* 30:2032–3.
16. Bregenholt S, et al. (2005) The long-acting glucagonlike peptide-1 analogue, liraglutide, inhibits beta-cell apoptosis in vitro. *Biochem. Biophys. Res. Commun.* 330:577–84.

17. Li L, *et al.* (2008) Exenatide prevents fat-induced insulin resistance and raises adiponectin expression and plasma levels. *Diabetes Obes. Metab.* 10:921–30.
18. Li K, *et al.* (2010) Effect of short hairpin RNA-mediated adiponectin/Acrp30 down-regulation on insulin signaling and glucose uptake in the 3T3-L1 adipocytes. *J. Endocrinol. Invest.* 33:96–102.
19. Ling L, *et al.* (2009) The adipose triglyceride lipase, adiponectin and visfatin are downregulated by tumor necrosis factor- α (TNF- α) in vivo. *Cytokine.* 45:12–9.
20. Steele R, Wall JS, DeBodo RC. (1956) Measurement of size and turnover rate of body glucose pool by the isotope dilution method. *Am. J. Physiol.* 187:15–24.
21. Yu C, Gangyi Y, Ling L, Ling K, Wenwen C. (2009) The changes of glucose-lipid metabolism in ApoE $^{-/-}$ mice with high-fat induced insulin resistance. *Chinese J. Diabetes.* 17:590–603.
22. Marshall BA, Hansen PA, Ensor NJ, Ogdan MA, Mueckler M. (1999) GLUT-1 or GLUT-4 transgenes in obese mice improve glucose tolerance but do not prevent insulin resistance. *Am. J. Physiol. Endocrinol. Metab.* 276:390–400.
23. Rothman DL, *et al.* (1995) Decreased muscle glucose transport/phosphorylation is an early defect in the pathogenesis of non-insulin-dependent diabetes mellitus. *Proc. Natl. Acad. Sci. U. S. A.* 92:983–7.
24. Postic C, Dentin R, Girard J. (2004) Role of the liver in the control of carbohydrate and lipid homeostasis. *Diabetes Metab.* 30:398–408.
25. Kraemer FB, Shen WJ. (2002) Hormone-sensitive lipase: control of intracellular tri-(di-) acylglycerol and cholesteryl ester hydrolysis. *J. Lipid Res.* 43:1585–94.
26. Zimmermann R, *et al.* (2003) Decreased fatty acid esterification compensates for the reduced lipolytic activity in hormone-sensitive lipase-deficient white adipose tissue. *J. Lipid Res.* 44:2089–99.
27. Laplante M, *et al.* (2003) PPAR- γ activation mediates adipose depot-specific effects on gene expression and lipoprotein lipase activity. *Diabetes.* 52:291–9.
28. Mandard S, Muller M, Kersten S. (2004) Peroxisome proliferator-activated receptor alpha target genes. *Cell. Mol. Life Sci.* 61:393–416.
29. Fu T, Mukhopadhyay D, Davidson NO, Borensztajn J. (2004) The peroxisome proliferator-activated receptor α (PPAR α) agonist ciprofibrate inhibits apolipoprotein B mRNA editing in low density lipoprotein receptor-deficient mice. *J. Biol. Chem.* 279:28662–9.
30. Krapivner S, *et al.* (2008) Insulin-induced gene 2 involvement in human adipocyte metabolism and body weight regulation. *J. Clin. Endocrinol. Metab.* 93:1995–2001.
31. Horton JD, Goldstein JL, Brown MS. (2002) SREBPs: activators of the complete program of cholesterol and fatty acid synthesis in the liver. *J. Clin. Invest.* 109:1125–31.
32. Yang T, *et al.* (2002) Crucial step in cholesterol homeostasis: sterols promote binding of SCAP to INSIG-1, a membrane protein that facilitates retention of SREBPs in ER. *Cell.* 110:489–500.
33. Yabe D, Brown MS, Goldstein JL. (2002) Insig-2, a second endoplasmic reticulum protein that binds SCAP and blocks export of sterol regulatory element-binding proteins. *Proc. Natl. Acad. Sci. U. S. A.* 99:12753–8.
34. Smith S, Witkowski A, Joshi AK. (2003) Structural and functional organization of the animal fatty acid synthase. *Prog. Lipid Res.* 42:289–317.